Microwave Absorption Performance of One-dimensional Mixed Metal Oxide Nanocomposite

Cong Wang[1], Liefu Li[2], Jingwei Li[3], Qingqing Wang[1], Jinze Cao[1] and Jianjun Li[1,*]

[1]National Key Laboratory of Science and Technology on Advanced Composites in Special Environments, Harbin Institute of Technology, Harbin, 150080, P. R. China

[2]China Energy Engineering Group Northeast No.1 Electric Power Construction Co., Ltd. Shenyang, 110000, P. R. China

[3]School of Materials Science and Engineering, Harbin Institute of Technology, Harbin, 150080, P. R. China

Abstract: Microwave-absorbing materials have received numerous attentions in terms of their key roles in the fields of stealth technology and controlling electromagnetic radiation pollution. In this paper, we aim to develop one-dimensional $CoFe_2O_4$-TiO_2 mixed metal oxide nanocomposite via combination of sol-gel method and electrospinning technique. and investigate its microwave absorbing capability. The phase evolution from precursor fiber to final product and corresponding micromorphology are characterized, and microwave absorption performance for different $CoFe_2O_4$-TiO_2 composite fibers are investigated with a vector network analyzer in 2-18 GHz. The prepared $CoFe_2O_4$-TiO_2 mixed metal oxide composite fibers exhibit excellent microwave absorbing ability. The low reflection loss can reach -32.8 dB, and the maximum effective bandwidth is up to 6 GHz (12-18 GHz) at the thickness of 4 mm. The results further reveal that the lightweight mixed metal oxide composite fiber is promising for applications in electromagnetic attenuation and other related research fields.

Keywords: Microwave absorption, Mixed metal oxide, Composite fiber.

1. INTRODUCTION

With rapid development of electronic science and technology, electromagnetic irradiation has resulted in serious environmental pollution and harmful effects on human health. The exploration of efficient microwave absorbers to attenuate electromagnetic energy and convert it into thermal energy has been receiving increasing attention. Researchers are focusing on seeking and designing microwave absorbing materials to satisfy the high-performance requirements of “thin thickness, low density, strong absorption and wide bandwidth” [1-7]. Consequently, tremendous efforts have been devoted to develop unique one-dimensional nanomaterials to enhance the microwave absorption performance.

One-dimensional nanofibers, nanowires and nanotubes, have attracted intensive interest because of their exceptional properties and wide applications in many research fields. Among the various methods to prepare such one-dimensional materials, electrospinning technique provides a simple, direct and relatively inexpensive route to produce one dimensional product with diameters ranging from a few nanometers to several micrometers [8-16]. The combination of sol-gel process and electrospinning has been employed to prepare one dimensional microwave absorbers, which can have intrinsic structure with the length in micrometer and the diameter of only a few nanometers, and possesses the features of low density and anisotropic behavior [17-24]. The Fe_3O_4 and Fe nanowires via partial and full reduction of α-Fe_2O_3 have successfully synthesized by electrospinning method and the Fe_3O_4 nanowires exhibit a minimum RL -17.2 dB at 6.2 GHz [25]. Iron-nickel alloy electrospun fibers have been synthesized through citric acid organic gel thermal reduction process and induced interfaces between alloy and oxide brings about more stable microwave absorption performance of product [26]. Also, nanofibrous absorber composed of flexible carbon nanofibers and magnetic oxide nanoparticles shows enhanced microwave absorption performance in a broad frequency range with smaller absorber layer thickness [27].

Interface coupling is one of the factors that play important contribution to the strong microwave absorption. In heterogeneous structures of composites, the components on the interface have different polarity or conductivity and can give rise to increase in dielectric loss. Thus, increased interfacial polarization relaxation can lead to the enhancement of microwave absorption properties. Broadband microwave absorption of Fe_3O_4 single bond $BaTiO_3$ composites enhanced by interfacial polarization and impedance matching has been investigated. And the results reveal that the composites remain as two distinct phases and two phases can form special interface [28]. Titanium dioxide (TiO_2) is not an ideal candidate for absorption of electromagnetic energy, but amorphous TiO_2 synthesized with partially crystallized displays strong

*Address correspondence to this article at the National Key Laboratory of Science and Technology on Advanced Composites in Special Environments, Harbin Institute of Technology, Harbin, 150080, P. R. China;
E-mail: ljj8081@gmail.com

microwave absorption ability [29]. Dielectric properties of TiO_2/Al_2O_3 ceramics are fabricated by APS technique and their microwave absorption properties are improved [30]. In this manuscript, lightweight $CoFe_2O_4$-TiO_2 mixed metal oxide composite fibers were prepared by a combination of the sol-gel and electrospinning techniques. Citric acid-based iron-cobalt precursor can be mixed with titanium dioxide sol homogeneously at the molecular level. Finally, in situ synthesized microwave absorption performance and mechanism of $CoFe_2O_4$-TiO_2 composite fiber are investigated. In this composite system, the magnetic $CoFe_2O_4$ contributes to the active magnetic loss, while the TiO_2 may support the dielectric loss. Compositions and the corresponding interface coupling are optimized to enhance its microwave absorption characters. The prepared $CoFe_2O_4$-TiO_2 composite fibers showcase remarkable performance in microwave absorbing. Achieving a low reflection loss of -32.8 dB and a maximum effective bandwidth of up to 6 GHz (within the 12-18 GHz range) with a thickness of 4 mm, this lightweight mixed metal oxides holds considerable potential for applications in electromagnetic attenuation and associated research.

2. EXPERIMENTAL PROCEDURE

$Fe(NO_3)_3 \cdot 9H_2O$ (98.5%), $Co(NO_3)_2 \cdot 6H_2O$ (99.0%) and citric acid (99.5%) are provided from Tianjin Chemical Company. Polyethylene oxide (PEO, Mn=900,000) from Changchun Jinghua Company was used as electrospinning carrier. Tetrabutyl titanate (TBT, 99%) is supplied by Aladdin Industrial Corporation. All chemicals reagents are used as received without further purification. In a typical synthesis of $CoFe_2O_4$ sol, 1.455g $Co(NO_3)_2 \cdot 6H_2O$, 4.04g $Fe(NO_3)_3 \cdot 9H_2O$, 5g citric acid, 15 ml ethanol and 7 ml distilled water are mixed and stirred to be homogeneous. TiO_2 sols for electrospinning were prepared by hydrolyzing Tetrabutyl titanate precursor. For the preparation of the TiO_2 sol, a 12 mL mixture containing ethanol, water and nitric acid is slowly added into a 65 mL solution of tetrabutyl titanate and ethanol (with a molar ratio of tetrabutyl titanate:ethanol = 1:9.2). Thus, electrospun precursor fibers with different molar ratio of $CoFe_2O_4$ to TiO_2 can be produced by electrospinning. In Sample M1, the molar ratio of $CoFe_2O_4$ to titanium dioxide is 2:1, while in Sample M2, the molar ratio of $CoFe_2O_4$ to titanium dioxide is 8:1. Lightweight $CoFe_2O_4$-TiO_2 mixed metal oxide composite fibers are prepared by heat-treatment of the electrospun precursor fibers.

In this experiment, a needle electrospinning apparatus, procured from Beijing Future Material Sci-tech Company, was utilized for the preparation of fibers. The electrospinning process involved setting the flow rate of mixtures at 0.03 mL/min, maintaining a needle-to-collector distance of 15 cm, and applying a voltage of 18 kV. Thermo-gravimetric and differential thermal analyses (TGA-DTA) were conducted using a Netzsch/STA499F3 thermo-gravimetric analyzer under both air and argon atmospheres. The powder X-ray diffraction (XRD) patterns were acquired using a

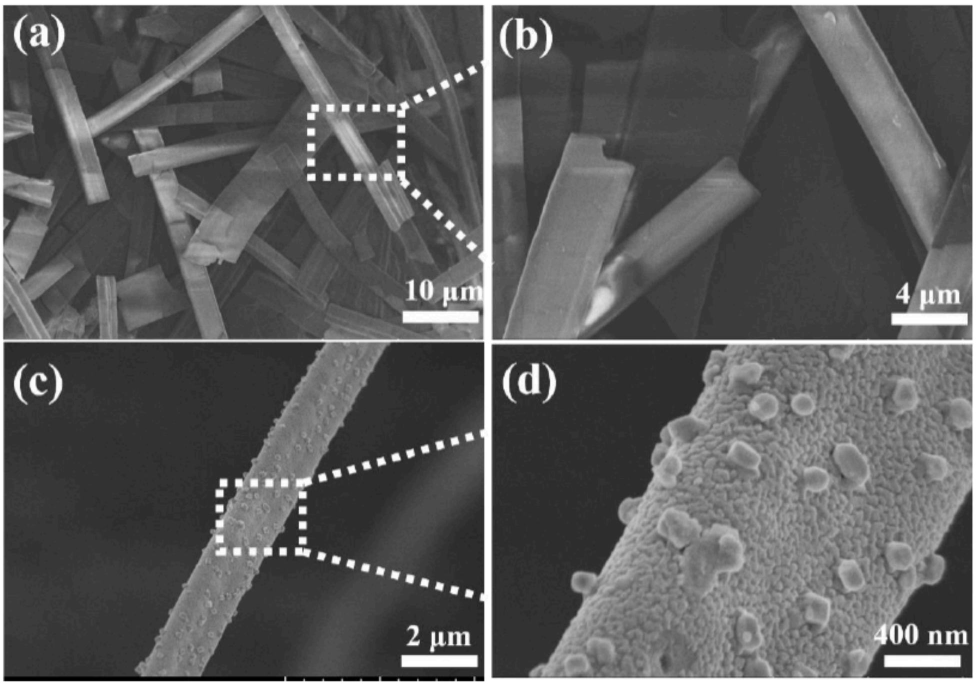

Figure 1: SEM images of $CoFe_2O_4$-TiO_2 mixed metal oxide composite fibers (**a**), (**b**) before and (**c**), (**d**) after processing in Sample M1 (the molar ratio of $CoFe_2O_4$ to titanium dioxide is 2:1).

diffractometer with Cu Kα radiation. Scanning Electron Microscope (SEM) images were captured using the HITACHI SU8000 equipment. Additionally, the energy-dispersive x-ray spectrometer (EDS, Bruker) was carried out, in order to assess the distribution patterns of elements in the nanocomposites. Relative permittivity and permeability were determined employing an HP-5783E vector network analyzer within the frequency range of 2-18 GHz for the precise calculation of reflection loss. The $CoFe_2O_4$-TiO_2 fibers/paraffin composites were meticulously prepared by uniformly mixing the nanofibers in a paraffin matrix. Subsequently, paraffin-based composite samples, comprising 15 wt% and 33 wt% of the prepared $CoFe_2O_4$-TiO_2 composite fibers, were compressed into a ring with an outer diameter of 7 mm, an inner diameter of 3 mm, and a thickness of 2 mm for the measurement of electromagnetic parameters.

3. RESULTS AND DISCUSSION

Figure **1** displays SEM images of oxide fibers in Sample M1 with an average major-axis diameter of 1.58 µm. And the SEM images elucidate the in-situ assembly process of oxide nanoparticles into a fibrous structure. The oxidation of Co–Fe particles on the nanofiber surface initiates the process. Subsequently, the carbon-based fiber undergoes gradual combustion, leading to the exposure and continuous oxidation of the metal particles until the reaction reaches completion. Ultimately, the fiber undergoes a transition from a smooth surface to rough one with nanoparticle. Figure **2** displays SEM images of oxide fibers in Sample M2. Similar to Sample M1, nanoparticles exhibit uniform growth on the fiber surface. An increased addition of titanium dioxide resulted in a reduction in the diameter of nanoparticles on the fiber surface. Specifically, an excessively high dosage of titanium dioxide adversely affected the nucleation of metal oxides. Examination of the samples through SEM confirms the presence of high-roughness surfaces adorned with nanoparticles (Figure **1**, **2**). The integration of high roughness surfaces and nanoparticles introduces multiple reflection points, thereby enhancing microwave dissipation.

To investigate the presence and distribution of Co, Fe, and Ti elements, EDS elemental mapping is employed to record the data in Sample M1. The mapping analysis depicted in Figure **3** confirm the homogeneous distribution of Co, Fe, and Ti elements. Co, Fe, and Ti elements are represented by purple (Figure **4b**), red (Figure **4c**), and green spots (Figure **4d**), respectively, evenly distributed throughout the scanned area.

For further confirmation, XRD patterns of the $CoFe_2O_4$/TiO_2(Sample M1) and $CoFe_2O_4$/TiO_2 (Sample M2) are recorded and shown in Figure **4**. The noticeable diffraction peaks correspond to the (200), (311), (400), (511) and (440) Miller indices of $CoFe_2O_4$, which could be observed in all samples. It is clear that Sample M1 and Sample M2 have different dominant

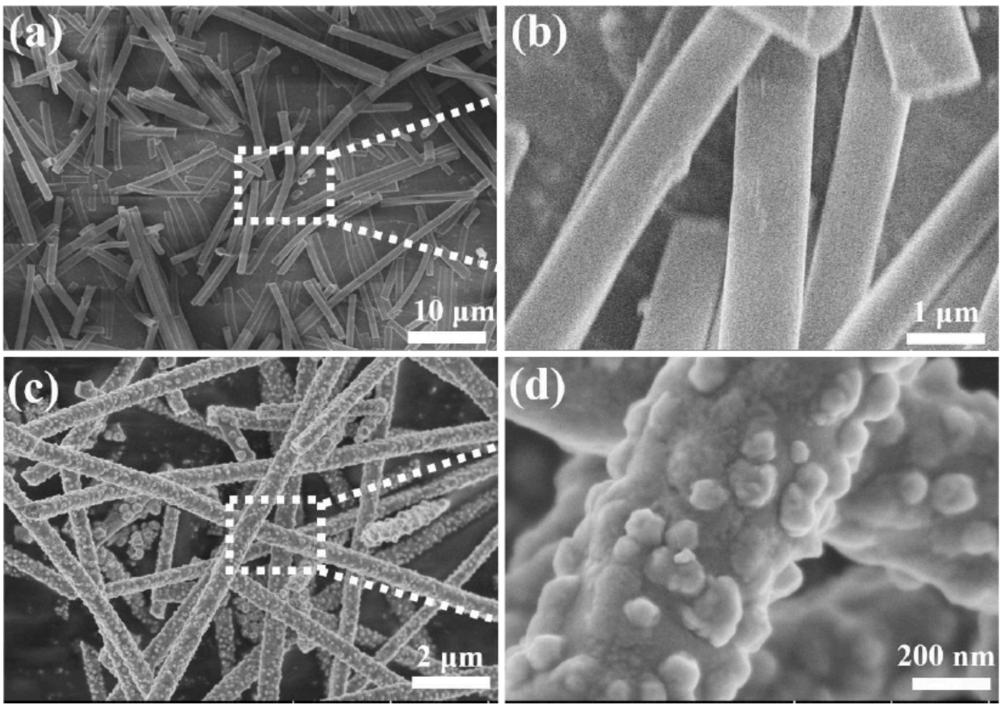

Figure 2: SEM images of $CoFe_2O_4$-TiO_2 mixed metal oxide composite fibers (**a**), (**b**) before and (**c**), (**d**) after processing in Sample M2 (the molar ratio of $CoFe_2O_4$ to titanium dioxide is 8:1).

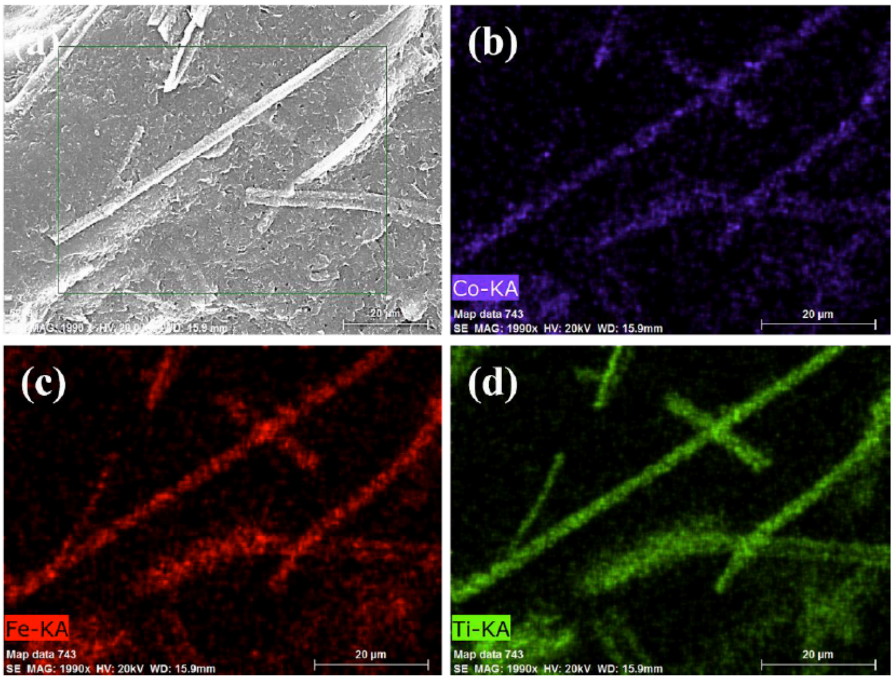

Figure 3: Elemental mapping analysis of Sample M1 (the molar ratio of $CoFe_2O_4$ to titanium dioxide is 2:1).

peaks. This phenomenon could be caused by the existence of TiO_2.

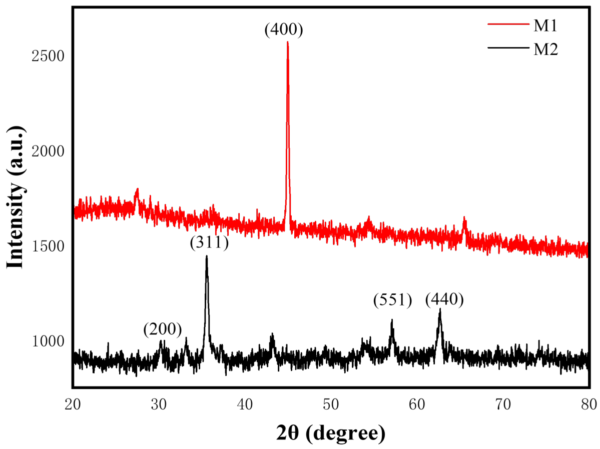

Figure 4: XRD diffraction patterns of the prepared samples: Sample M1(the molar ratio of $CoFe_2O_4$ to titanium dioxide is 2:1) and Sample M2(the molar ratio of $CoFe_2O_4$ to titanium dioxide is 8:1).

In order to further investigate the changes during sample preparation, Thermogravimetric Analysis (TG) and Differential Thermal Analysis (DTA) are introduced. Figure **5** show the TG-DTA curves of the $CoFe_2O_4/TiO_2$ samples. The samples in different ratios exhibits a similar mass loss trend and two major quality losses occurred at 35-80 °C and 150-310 °C, respectively. Similarly, exothermal peaks are observed at corresponding positions in the DTA curve. The first step can be attributed to solvent volatilization, while the second is due to the decomposition of organic matter in the solvent. After 310 °C, only a small amount of quality loss occurs. It is worth noting that the remaining mass of Samples M1 and M2, is 27% and 12% respectively which is due to the different degrees of organic matter decomposition decomposed caused by the different amounts of citric acid.

The complex permittivity ($\varepsilon_r = \varepsilon' - j\varepsilon''$) and complex permeability ($\mu_r = \mu' - j\mu''$) are introduced to

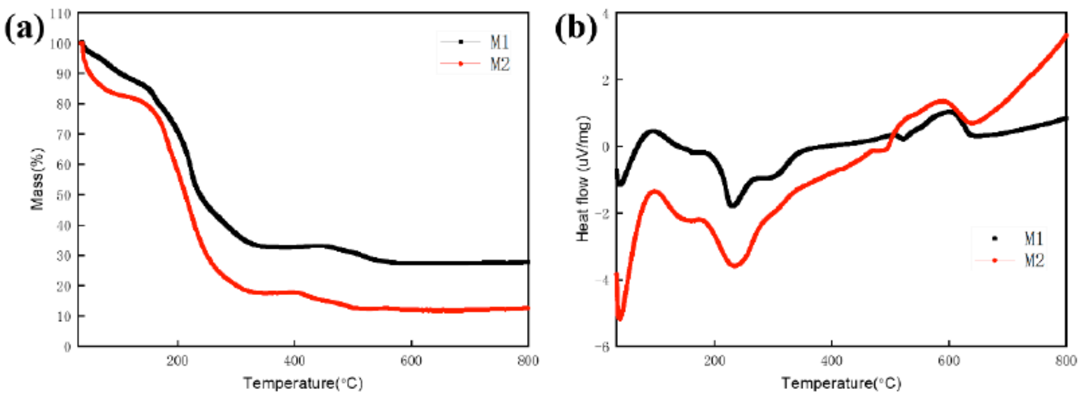

Figure 5: (**a**) TG and (**b**) DTA curves of $CoFe_2O_4$-TiO_2 mixed metal oxide composite fiber samples.

determine the attenuation of the electric and magnetic fields. Figure **6** (**a**), (**b**) show ε' and ε'' for paraffin-based samples in the 2-18 GHz and both ε' and ε'' of Sample M1 are higher than those of Sample M2. At f=2 GHz, ε′ (=7.78) and ε″ (=4.78) of Sample M1 are much higher than that of Sample M2 (ε′=3.00, ε″=0.008). Subsequently, ε' and ε'' of Sample M1 are slightly increased with the increase in frequency. While ε' and ε″ of Sample M2 remain constant. The attenuation of the electric field is evaluated through the dielectric loss tangents by using the expression as $\tan\delta_\varepsilon$ = ε″/ε′. The dielectric loss tangent ($\tan\delta_\varepsilon$) curve is shown in Figure **6**(**c**). It is worth noticing that the $\tan\delta_\varepsilon$ values of Sample M1 are all higher than those of Sample M2, which would play a critical role in microwave absorbing.

μ' and μ'' of the samples are displayed in Figure **6**(**d**), (**e**) ,respectively. When the μ' and μ″ curves of $CoFe_2O_4/TiO_2$ samples are compared, these values are mostly the same in the range of 2-18 GHz. However, $CoFe_2O_4$/TiO2 samples have relatively higher μ' and lower μ″ which could be attributed to the introduction of TiO_2 bringing additional interfaces. The magnetic loss $\tan\delta_\mu$ ($\tan\delta_\mu$ = μ″/μ′) indicating the attenuation of magnetic field is shown in Figure **6** (**f**). The $\tan\delta_\mu$ curves of $CoFe_2O_4/TiO_2$ samples are similar, with less differences compared with $\tan\delta_\varepsilon$ curves. Therefore, the microwave dissipation characteristics of the material are mainly determined by $\tan\delta_\varepsilon$.

The reflection loss reflects the absorbance ability of the samples.According to transmission line theory, the reflection loss in decibels (dB) of electromagnetic radiation when it is normally incident upon the surface of a single-layer material backed by a perfect conductor can be expressed as follows:

$$RL(dB) = 20\lg\left|\frac{Z_{in}-Z_0}{Z_{in}+Z_0}\right| \quad (1)$$

where Z_0 is the characteristic impedance of free space,

$$Z_0 = \sqrt{\frac{\mu_0}{\varepsilon_0}} \quad (2)$$

Z_{in} is the input impedance at the interface of free space and material,

$$Z_{in} = Z_0\sqrt{\frac{\mu_r}{\varepsilon_r}}\tanh\left[j\frac{2\pi f d}{c}\sqrt{\mu_r\varepsilon_r}\right] \quad (3)$$

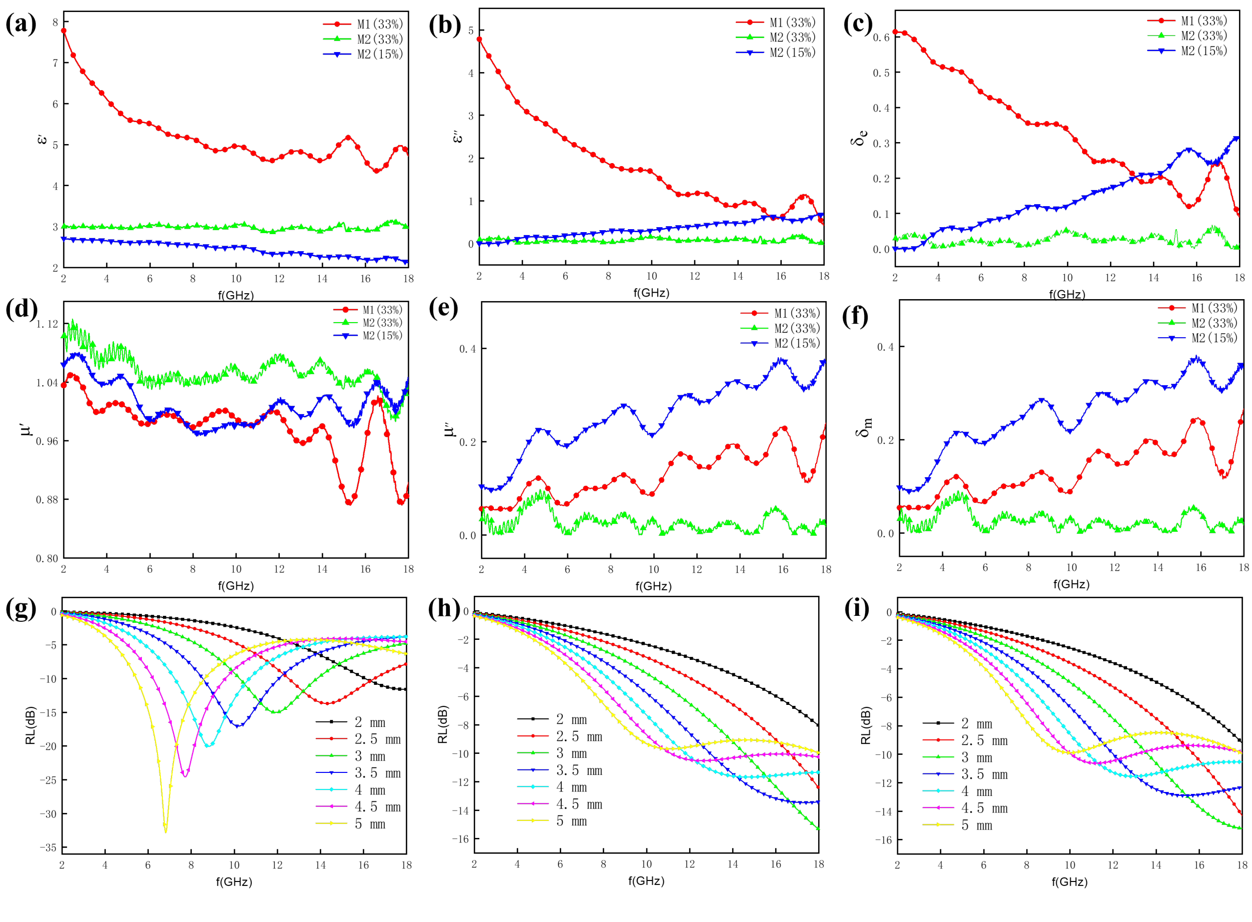

Figure 6: (**a**) Real, (**b**) imaginary permittivity, (**c**) dielectric loss tangent ($\tan\delta_\varepsilon$), (**d**) real and (**e**) imaginary permeability, (**f**) magnetic loss tangent ($\tan\delta_\mu$), RL curves of different absorbers :(**g**) Sample M1(33%), (**h**)Sample M2(15%), (**i**) Sample M2(33%) of paraffin-based samples in the frequency range of 2–18 GHz.

where f is the frequency of the EM wave, d is the thickness of the material, ε is the relative permittivity and μ is relative permeability.

Figure **6**(**g**), (**h**), (**i**) depict the RL curves of single-layer paraffin based $CoFe_2O_4/TiO_2$ absorbers with t=2-5 mm (increments of 0.5 mm). Sample M1 demonstrates the most effective electromagnetic wave absorption capability when compared to other samples. The low reflection loss can reach -32.8 dB, and the maximum effective bandwidth is up to 6 GHz (12-18 GHz) at the thickness of 4 mm. Sample M2 with different absorber content exhibits similar electromagnetic wave absorption capability with a RL_{max} of -15 dB at 18GHz with the thickness of 3 mm. Primarily, the advantageous interfacial polarization for microwave attenuation arises from the presence of multi-interfaces. Secondly, the considerable specific surface areas and high porosities are facilitated by TiO_2 and the void space between $CoFe_2O_4$ and TiO_2 providing ample active sites for microwave reflection and scattering. Lastly, the interruption of electromagnetic wave propagation is achieved with the addition of TiO_2, effectively generating dissipation due to impedance differences.

4. CONCLUSIONS

In this paper, $CoFe_2O_4$-TiO_2 mixed metal oxide composite fibers were successfully prepared with different molar ratios of $CoFe_2O_4$ to titanium dioxide. The physicochemical characteristics of composite fibers were investigated through SEM, EDS, XRD, TG/DTA. The XRD patterns indicate main diffraction peaks of $CoFe_2O_4$ could be observed in all samples. TG and DTA curves reveal that the samples in different ratios exhibits similar mass loss trend. The electromagnetic properties of the paraffin-based Samples M1 and M2 were studied in the 2–18 GHz frequency range, which showed that the prepared $CoFe_2O_4$-TiO_2 mixed metal oxide composite fibers exhibit excellent microwave absorbing ability. The low reflection loss can reach -32.8 dB, and the maximum effective bandwidth is up to 6 GHz (12-18 GHz) at the thickness of 4 mm. The composite fiber composed of lightweight mixed metal oxides shows great promise for utilization in electromagnetic attenuation and various related research domains.

DECLARATION OF COMPETING INTEREST

The authors declare that they have no known competing financial interests or personal relationships that could have appeared to influence the work reported in this paper.

ACKNOWLEDGEMENTS

This work was supported by Funding of Science and Technology on Advanced Composites in Special Environment Laboratory, State Key Laboratory of Mechanics and Control of Mechanical Structures (Nanjing University of Aeronautics and astronautics) (Grant No. MCMS-E-0522G03).

REFERENCES

[1] QIN M, LIANG H S, ZHAO X R, *et al*. Filter paper templated one-dimensional NiO/NiCoO microrod with wideband electromagnetic wave absorption capacity. Journal of Colloid and Interface Science, 2020, 566: 347-356. https://doi.org/10.1016/j.jcis.2020.01.114

[2] CHEN Z H, TIAN K H, ZHANG C, *et al*. In-situ hydrothermal synthesis of NiCo alloy particles@hydrophilic carbon cloth to construct corncob-like heterostructure for high-performance electromagnetic wave absorbers. Journal of Colloid and Interface Science, 2022, 616: 823-833. https://doi.org/10.1016/j.jcis.2022.02.086

[3] LI B B, MAO B X, WANG X B, *et al*. Novel, hierarchical SiC nanowire-reinforced SiC/carbon foam composites: Lightweight, ultrathin, and highly efficient microwave absorbers. Journal of Alloys and Compounds, 2020, 829. https://doi.org/10.1016/j.jallcom.2020.154609

[4] WANG Z Q, ZHAO P F, LI P W, *et al*. Hierarchical cerium oxide anchored multi-walled carbon nanotube hybrid with synergistic effect for microwave attenuation. Composites Part B-Engineering, 2019, 167: 477-486. https://doi.org/10.1016/j.compositesb.2019.03.018

[5] ZHAO Y, ZHANG H, YANG X, *et al*. In situ construction of hierarchical core–shell Fe_3O_4@C nanoparticles–helical carbon nanocoil hybrid composites for highly efficient electromagnetic wave absorption. Carbon, 2021, 171: 395-408. https://doi.org/10.1016/j.carbon.2020.09.036

[6] KONG L, LUO S H, ZHANG G Q, *et al*. Interfacial polarization dominant CNTs/PyC hollow microspheres as a lightweight electromagnetic wave absorbing material. Carbon, 2022, 193: 216-229. https://doi.org/10.1016/j.carbon.2022.03.016

[7] GUAN G, YAN L, ZHOU Y, *et al*. Composition design and performance regulation of three-dimensional interconnected FeNi@carbon nanofibers as ultra-lightweight and high efficiency electromagnetic wave absorbers. Carbon, 2022, 197: 494-507. https://doi.org/10.1016/j.carbon.2022.07.005

[8] LI D R, GUO K, WANG F Y, *et al*. Enhanced microwave absorption properties in C band of Ni/C porous nanofibers prepared by electrospinning. Journal of Alloys and Compounds, 2019, 800: 294-304. https://doi.org/10.1016/j.jallcom.2019.05.284

[9] YANG J, GUAN G, XIANG J, *et al*. Electrospinning fabrication and enhanced microwave absorption properties of nickel porous nanofibers. Journal of Alloys and Compounds, 2022, 891. https://doi.org/10.1016/j.jallcom.2021.161997

[10] JIANG Y L, FU X Y, ZHANG Z D, *et al*. Enhanced microwave absorption properties of FeC/C nanofibers prepared by electrospinning. Journal of Alloys and Compounds, 2019, 804: 305-313. https://doi.org/10.1016/j.jallcom.2019.07.038

[11] WANG P, CHENG L, ZHANG Y, *et al*. Electrospinning of graphite/SiC hybrid nanowires with tunable dielectric and microwave absorption characteristics. Composites Part A: Applied Science and Manufacturing, 2018, 104: 68-80. https://doi.org/10.1016/j.compositesa.2017.10.012

[12] LI L, CHEN Z, PAN F, *et al*. Electrospinning technology on one dimensional microwave absorbers: fundamentals, current progress, and perspectives. Chemical Engineering

Journal, 2023, 470.
https://doi.org/10.1016/j.cej.2023.144236

[13] WANG F Y, SUN Y Q, LI D R, *et al*. Microwave absorption properties of 3D cross-linked Fe/C porous nanofibers prepared by electrospinning. Carbon, 2018, 134: 264-273.
https://doi.org/10.1016/j.carbon.2018.03.081

[14] HAN C, ZHANG M, CAO W Q, *et al*. Electrospinning and in-situ hierarchical thermal treatment to tailor C-NiCoO nanofibers for tunable microwave absorption. Carbon, 2021, 171: 953-962.
https://doi.org/10.1016/j.carbon.2020.09.067

[15] ZHANG Z Y, ZHAO Y H, LI Z H, *et al*. Synthesis of carbon/SiO core-sheath nanofibers with Co-Fe nanoparticles embedded in via electrospinning for high-performance microwave absorption. Advanced Composites and Hybrid Materials, 2022, 5(1): 513-524.
https://doi.org/10.1007/s42114-021-00350-w

[16] HOU Y, CHENG L F, ZHANG Y I, *et al*. Electrospinning of Fe/SiC Hybrid Fibers for Highly Efficient Microwave Absorption. Acs Applied Materials & Interfaces, 2017, 9(8): 7265-7271.
https://doi.org/10.1021/acsami.6b15721

[17] WANG C, LIU Y, JIA Z, *et al*. Multicomponent Nanoparticles Synergistic One-Dimensional Nanofibers as Heterostructure Absorbers for Tunable and Efficient Microwave Absorption. Nano-Micro Letters, 2022, 15(1).
https://doi.org/10.1007/s40820-022-00986-3

[18] LUO K, ZHAO B, XU C, *et al*. Construction of one-dimensional hierarchical MoS2/Ni3S2 composites with enhanced interfacial polarization and improved wideband microwave absorption. Journal of Materials Science & Technology, 2024, 178: 22-28.
https://doi.org/10.1016/j.jmst.2023.08.044

[19] LIAO Z J, MA M L, BI Y X, *et al*. MoS decorated on one-dimensional MgFeO/MgO/C composites for high-performance microwave absorption. Journal of Colloid and Interface Science, 2022, 606: 709-718.
https://doi.org/10.1016/j.jcis.2021.08.056

[20] JIAO Z, HU J, MA M, *et al*. One-dimensional core-shell CoC@CoFe/C@PPy composites for high-efficiency microwave absorption. Journal of Colloid and Interface Science, 2023, 650: 2014-2023.
https://doi.org/10.1016/j.jcis.2023.07.072

[21] BI Y X, MA M L, LIAO Z J, *et al*. One-dimensional Ni@Co/C@PPy composites for superior electromagnetic wave absorption. Journal of Colloid and Interface Science, 2022, 605: 483-492.
https://doi.org/10.1016/j.jcis.2021.07.050

[22] GUO S N, ZHANG Y Q, CHEN J B, *et al*. The excellent electromagnetic wave absorbing properties of carbon fiber composites: the effect of metal content. Inorganic Chemistry Frontiers, 2022, 9(13): 3244-3250.
https://doi.org/10.1039/D2QI00854H

[23] SUN M X, XIONG Z M, ZHANG Z W, *et al*. One-dimensional Ag@NC-Co@NC composites with multiphase core-shell hetero-interfaces for boosting microwave absorption. Composites Science and Technology, 2022, 228.
https://doi.org/10.1016/j.compscitech.2022.109663

[24] WANG Y-F, ZHU L, HAN L, *et al*. Recent Progress of One-Dimensional Nanomaterials for Microwave Absorption: A Review. ACS Applied Nano Materials, 2023, 6(9): 7107-7122.
https://doi.org/10.1021/acsanm.3c00818

[25] HAN R, LI W, PAN W, *et al*. 1D Magnetic Materials of Fe_3O_4 and Fe with High Performance of Microwave Absorption Fabricated by Electrospinning Method. Scientific Reports, 2014, 4(1).
https://doi.org/10.1038/srep07493

[26] WEI Z L, YANG S, JIAO P Z, *et al*. Novel and effective strategy for producing NiFe alloy fibers with tunable microwave absorption performance. Materialia, 2019, 8.
https://doi.org/10.1016/j.mtla.2019.100495

[27] ABDALLA I, SHEN J L, YU J Y, *et al*. CoO/carbon composite nanofibrous membrane enabled high-efficiency electromagnetic wave absorption. Scientific Reports, 2018, 8.
https://doi.org/10.1038/s41598-018-30871-2

[28] HUANG Y, JI J, CHEN Y, *et al*. Broadband microwave absorption of Fe_3O_4-$BaTiO_3$ composites enhanced by interfacial polarization and impedance matching. Composites Part B: Engineering, 2019, 163: 598-605.
https://doi.org/10.1016/j.compositesb.2019.01.008

[29] DONG J, ULLAL R, HAN J, *et al*. Partially crystallized TiO_2 for microwave absorption. Journal of Materials Chemistry A, 2015, 3(10): 5285-5288.
https://doi.org/10.1039/C4TA05908E

[30] YANG Z, LUO F, HU Y, *et al*. Dielectric and microwave absorption properties of TiO_2/Al_2O_3 coatings and improved microwave absorption by FSS incorporation. Journal of Alloys and Compounds, 2016, 678: 527-532.
https://doi.org/10.1016/j.jallcom.2016.04.031

Received on 08-11-2023 Accepted on 15-12-2023 Published on 26-12-2023

DOI: https://doi.org/10.31875/2410-4701.2023.10.13